Role of the Carbon-Based Gas Diffusion Layer on Flooding in a Gas Diffusion Electrode Cell for Electrochemical CO2 Reduction

Yang, Kailun; Kas, Recep; Smith, Wilson A.; Burdyny, Thomas

DOI
10.1021/acsenergylett.0c02184

Publication date
2021

Document Version
Final published version

Published in
ACS Energy Letters

ACS Energy LETTERS

http://pubs.acs.org/journal/aelccp

Role of the Carbon-Based Gas Diffusion Layer on Flooding in a Gas Diffusion Electrode Cell for Electrochemical CO_2 Reduction

Kailun Yang, Recep Kas, Wilson A. Smith, and Thomas Burdyny*

Cite This: *ACS Energy Lett.* 2021, 6, 33–40

Read Online

ACCESS | Metrics & More | Article Recommendations | Supporting Information

ABSTRACT: The deployment of gas diffusion electrodes (GDEs) for the electrochemical CO_2 reduction reaction (CO2RR) has enabled current densities an order of magnitude greater than those of aqueous H cells. The gains in production, however, have come with stability challenges due to rapid flooding of GDEs, which frustrate both laboratory experiments and scale-up prospects. Here, we investigate the role of carbon gas diffusion layers (GDLs) in the advent of flooding during CO2RR, finding that applied potential plays a central role in the observed instabilities. Electrochemical characterization of carbon GDLs with and without catalysts suggests that the high overpotential required during electrochemical CO2RR initiates hydrogen evolution on the carbon GDL support. These potentials impact the wetting characteristics of the hydrophobic GDL, resulting in flooding that is independent of CO2RR. Findings from this work can be extended to any electrochemical reduction reaction using carbon-based GDEs (CORR or N_2RR) with cathodic overpotentials of less than −0.65 V versus a reversible hydrogen electrode.

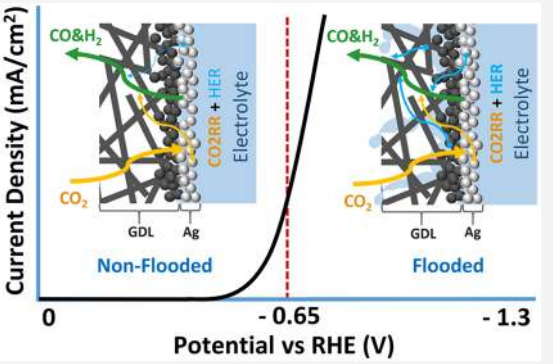

Carbon dioxide electrolysis is a technology with the potential to convert the most prevalent greenhouse gas into chemical feedstocks and fuels using renewable electricity.[1−3] As the field has advanced, it is clear that the reaction must occur at elevated reaction rates (e.g., high current densities), which has led to catalysts being positioned near a gas−liquid interface. This is typically achieved by using a gas diffusion electrode (GDE), where a catalyst is deposited on a gas diffusion layer (GDL).[4−6] Such application boosts the limiting CO_2 reduction current density by more than an order of magnitude when compared with that of electrodes in a conventional H cell that are typically limited to current densities of <60 mA/cm^2.[6−10]

A typical GDL consists of a porous matrix capable of allowing gas transport but limiting the transport of liquids.[11] GDLs have been employed for many systems and reactions such as fuel cells,[12] chlor-alkali electrolysis with oxygen-depolarized cathodes,[13] and most recently CO_2 electrolysis. In CO_2 electrolysis, various GDLs have been tested, including carbon-based,[14] metal-based,[15,16] PTFE-based,[17] and membrane-based structures.[18] Among those, carbon-based GDLs are the most prevalently reported in the literature,[6,7] with hydrophobicity imposed within a carbon matrix via PTFE coating. Unfortunately, the research community has shown that despite the excellent stability of carbon-based GDLs for other electrochemical reactions, in CO_2 reduction they suffer from extremely poor stability. In fact, flooding of the GDL will typically happen within several hours of operation, leading to a reduction in selectivity toward CO_2 reduction reaction products.[19−21] When flooding happens, a fraction of the pores within the originally hydrophobic GDL become filled by liquid. The penetration by water of the GDL not only blocks CO_2 from reaching the active site on the catalyst surface by increasing the diffusion pathway but also can encourage salt precipitation, which causes further failure by blocking the pore permanently. Thus, when flooding occurs, the performance becomes characterized by a switch in selectivity toward the hydrogen evolution reaction (HER), leading to an essential failure of the CO_2 electrolysis system.

Despite the recent increase in GDL usage for CO_2 electrolysis, the instability of these structures, especially flooding, is a well-studied phenomenon in fuel cell research.[22,23] Several flooding mechanisms have been pre-

Received: October 12, 2020
Accepted: November 20, 2020

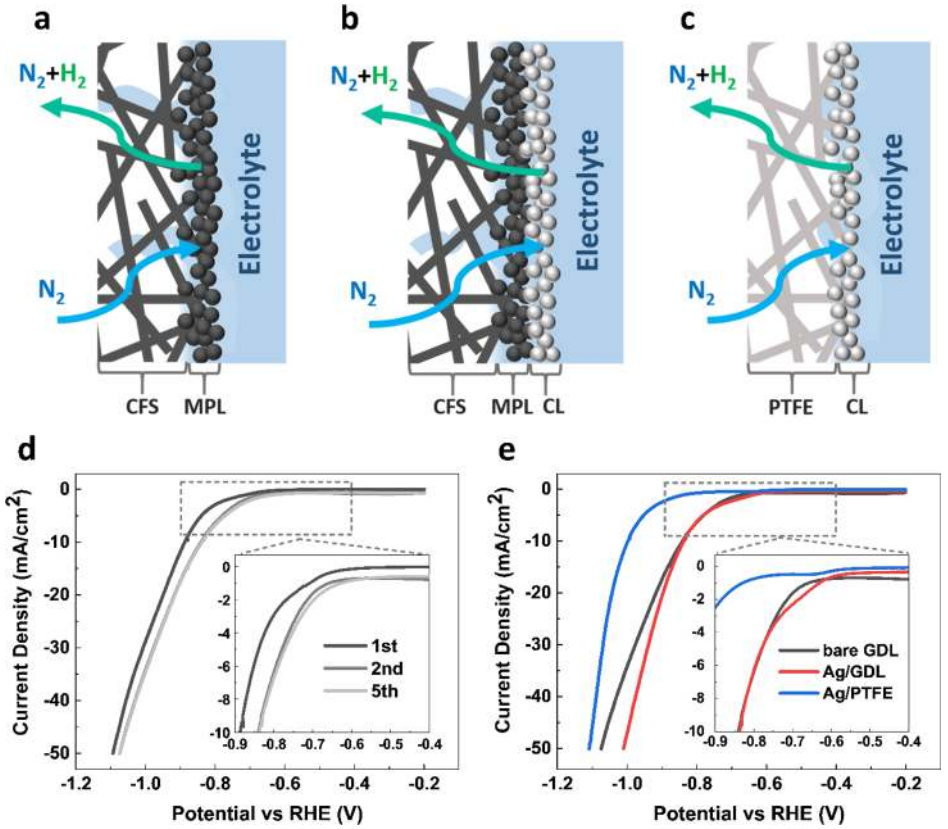

Figure 1. Illustration of the (a) bare GDL, (b) Ag/GDL, and (c) Ag/PTFE. (d) Multiple scans of linear scan voltammetry (LSV) of a bare carbon GDL performed under N_2 conditions. (e) Comparison of the second LSV scans for the GDL configurations shown in panels a−c. The insets in panels d and e show the enlarged rectangle regions. CFS represents carbon fiber substrate; MPL represents a microporous layer (which contains a mixture of carbon nanoparticles and PTFE), and CL represents a catalyst layer. All LSV scans used a scan rate of 10 mV/s in 1 M $KHCO_3$.

viously described, including electrowetting caused by a potential-driven change in the electrolyte−solid surface tension,[19,24,25] water pumping due to ion concentration gradients between the reaction interface and a bulk electrolyte,[24,26,27] salt precipitation due to ion build-up,[24,26] and pressure differences between the gas and liquid at the interface.[19,20,25−27] CO2RR-specific flooding mechanisms have also received attention. In a recent work, Leonard et al. found that in a KOH electrolyte, flooding can be related to the total charge passed on electrodes, leading to salt precipitation after sufficient CO_2/OH^- interactions.[21] Moreover, liquid products such as alcohols from CO2RR can further accelerate flooding as they tend to decrease the electrolyte−electrode surface tension of GDE, lowering the capillary pressure.[28] Lastly, Jouny et al. also observed flooding in an electrochemical CO reduction reaction (CORR) system when using KOH as an electrolyte, which they attributed to the condensation of water vapor.[29]

However, while different flooding mechanisms are possible over long-term electrochemical operation, there has not been a clear reason why flooding occurs almost immediately during CO_2 electrolysis, typically within 1 h.[21] In other words, can we understand why carbon-based GDEs used in so many other applications do not perform as advertised in the growing field of CO_2 electrolysis? Understanding such effects could help to provide a solution that not only impacts the future commercialization potential of CO2RR technology but also allows for greater ease to perform necessary long-term lab experiments on product selectivity and catalyst stability.[30]

In this work, we aim to elucidate the electrochemical factors leading to premature flooding of carbon-based gas diffusion layers during CO_2 electrolysis. We begin by investigating the electrochemical behavior of a bare carbon-based GDL, a silver catalyst on a carbon GDL, and a silver catalyst on a PTFE-based GDL in a CO_2-free reaction environment to decouple the roles of HER and CO2RR. After noting a large activity difference for HER between carbon- and silver-coated GDLs, we studied the electrochemical activity of a bare carbon GDL itself by comparison of other catalysts (Ag, Pt, Au, and Cu) on the same support. With regard to premature flooding, the GDL stability (e.g., resistivity to flooding) is subsequently found to be dependent on the potential applied and the corresponding electrochemical activity of the carbon on the GDL. The primary conclusion of our work is that by reducing the catalyst onset potentials and operating in a suitable potential range, CO_2 electrolyzers can reach a longer lifetime before flooding occurs. Such stability would greatly improve both the usability of GDLs for testing CO_2 electrolysis catalysts and operation, as well as enabling stability for industrial application.

To investigate the effect of electrochemical reactions on premature GDL flooding, one approach is to decouple each part of the reaction process (i.e., GDL vs catalyst and HER vs CO2RR). Here, we used three different electrodes to decouple these effects: a bare carbon-based GDL [containing a carbon−PTFE microporous layer (Figure 1a)], Ag deposited on this

https://dx.doi.org/10.1021/acsenergylett.0c02184
ACS Energy Lett. 2021, 6, 33−40

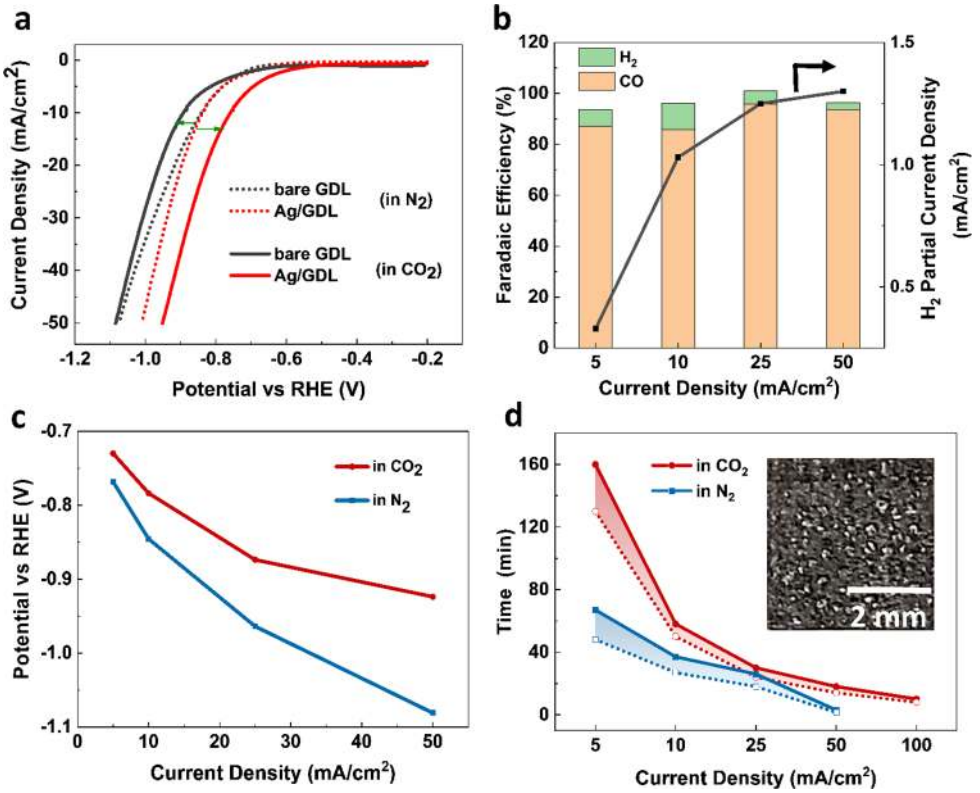

Figure 2. (a) Comparison of second LSVs on bare GDL and Ag/GDL in N_2 and CO_2 atmospheres. (b) FE (left) and partial current density to H_2 on Ag/GDL during CO2RR at different current densities. (c) Potentials needed during CO_2 and N_2 conditions at different current densities. (d) Time when flooding happened. Empty circles represent times when liquid droplets started to be observed. Solid circles represent times when GDE was totally flooded. The inset shows the image of a totally flooded sample. Current densities in (b), (c), and (d) represent cathodic current densities.

carbon-based GDL (Figure 1b), and Ag deposited on a PTFE-based GDL [a membrane made of PTFE (Figure 1c)]. Figure 1d shows the linear scan voltammetry (LSV) performed on a bare carbon GDL under a N_2 atmosphere in 1 M $KHCO_3$. In the first scan, the Faradaic onset potential is observed at −0.7 V versus a reference hydrogen electrode (RHE) (using −1 mA/cm^2 as the defining current density), with the corresponding electrochemical activity confirmed to be H_2 evolution. During the second scan, the onset potential for HER is then observed to shift to more anodic potentials (−0.65 V vs RHE). Upon repeated scans, the shape of the curve remains similar. The shift to anodic potentials indicates an increase in electrochemical activity. This may be due to the greater surface area of carbon in contact with the electrolyte, which is induced by the increased level of wetting of accessible carbon surfaces under an applied potential.[24] These results indicate that the bare carbon GDL is active for HER once it is in direct contact with the electrolyte and the applied potential is negative enough. Of note is the fact that the applied potentials are within the commonly reported potential range for CO_2 electrolysis.

Figure 1e shows an LSV sweep of a Ag/GDL, where a thin layer of Ag was deposited via magnetron sputtering on the carbon GDL (Figure 1b and Figure S2). Notably, the Ag/GDL and bare GDL have similar onset potentials and activity for HER within the potential range of −0.85 to −0.6 V versus RHE, indicating little difference in electrochemical activity between the two samples within this potential range. At more negative potentials (less than −0.85 V vs RHE), the activity of the Ag/GDL then becomes greater than that of the bare GDL.

To further investigate the role of Ag itself, we deposited Ag on a PTFE membrane, which has been used as a gas diffusion substrate for CO_2 electrolysis.[10,17,31] LSVs in Figure 1e show that Ag has a higher overpotential and a lower activity in the scanned potential window (−1.1 to −0.2 V vs RHE), compared with the bare carbon GDL under neutral pH conditions (1 M $KHCO_3$). Furthermore, the difference in HER activity between the bare GDL and the Ag/GDL can be explained by the activity of the Ag/PTFE sample, where the activity of carbon is removed. To rule out the influence of the different surface roughness of the carbon-based and PTFE-based GDLs (Figure S2), we normalized the current densities in Figure 1e to the electrochemical surface area (ECSA) current densities (Figure S5). After normalization, pure Ag on a PTFE substrate still gives the lowest performance for HER among the bare GDL, Ag/GDL, and Ag/PTFE electrodes. The results in Figure 1 conclude that during electrochemistry in a N_2 environment, carbon is a more active catalyst than Ag for HER (in the tested potential windows), and a substantial fraction of the Faradaic reactions could be electrochemically driven by the carbon GDL instead of Ag.

When the atmosphere is changed from N_2 to CO_2, the LSV scans (Figure 2a) show that the Ag/GDL sample has a smaller overpotential and a higher activity when compared to those for the same catalyst in a N_2 environment or to those of the the bare GDL. Conversely, the activity of the bare GDL is reduced under a CO_2 atmosphere compared to when it was under N_2 at lower current densities. Such observations could be explained by Zhang et al. showing that co-adsorbed CO from CO2RR

https://dx.doi.org/10.1021/acsenergylett.0c02184
ACS Energy Lett. 2021, 6, 33−40

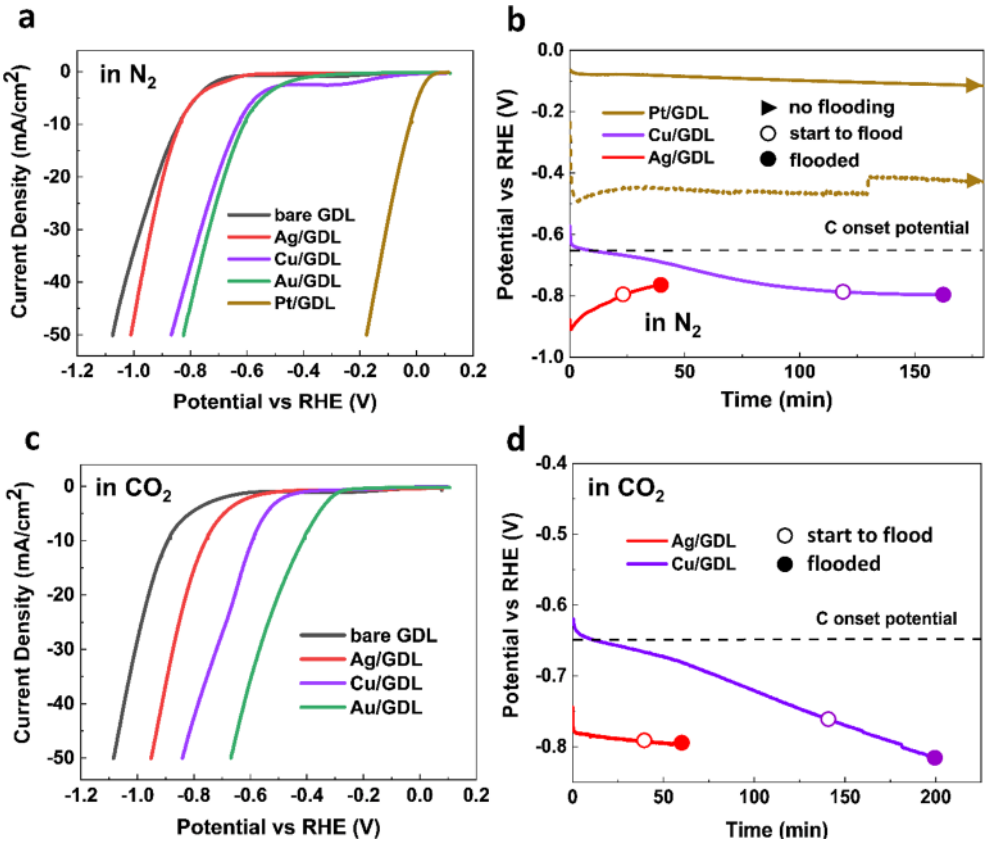

Figure 3. LSVs on different catalysts deposited onto a carbon GDL in 1 M $KHCO_3$ and (a) a N_2 reaction environment and (c) a CO_2 reaction environment. (b) Potentials and time when flooding happened on Ag/GDL, Cu/GDL, and Pt/GDL samples at 10 mA/cm^2 in a N_2 environment (dotted line shows 50 mA/cm^2 on Pt). (d) Potentials and time when flooding happened on Ag/GDL and Cu/GDL samples at 10 mA/cm^2 in a CO_2 environment. Empty circles indicate droplet observation on the back of the GDL. Filled circles indicate droplets across the entire back of the GDL. The dashed line shows the onset potential of carbon defined at −1 mA/cm^2 taken from the LSV curves.

will decrease the binding energy between adsorbed H and the catalyst surface, which suppresses hydrogen formation.[32]

When performing chronopotentiometry of the Ag/GDL sample in a CO_2 environment at various current densities, we observe that hydrogen is always measured (Figure 2b). Further, the partial current density toward H_2 (right *y*-axis) increases as the total current/potential increases. Pairing the applied potentials (Figure 2c) with the LSV curves of the bare GDL (Figure 2a), we hypothesize that a portion of the H_2 production observed on the Ag/GDL sample (Figure 2b) could originate from the carbon substrate. The carbon GDL, which is meant to play a passive electrochemical role, is then active toward the competing electrochemical reaction. Figure 2c shows the potentials corresponding to the different current densities under CO_2 and N_2 conditions during chronopotentiometry. At the same current density, the measured potential in a CO_2 atmosphere is less negative than under N_2 conditions due to the better kinetics for CO2RR than HER on Ag/GDL (shown in Figure 2a). Under CO_2 conditions, however, the potentials are still great enough that carbon can be active for HER (less than −0.65 V vs RHE).

During the chronopotentiometry measurements, we also observed the time taken for initial and full flooding of the GDL in both N_2 and CO_2 environments using a Ag/GDL (Figure 2d). There are two takeaways from these experiments. (1) At all current densities, flooding was observed to happen faster in a N_2 environment than in a CO_2 environment, and (2) in both the CO_2 and N_2 environments, the time to flooding decreased as current densities were increased. At 50 mA/cm^2, for example, liquid droplets were observed across the back of the entire GDL after only 3 min in a N_2 environment, and approximately 20 min in a CO_2 environment (Figure S11). As carbon is expected to be the primary active catalyst for HER in a N_2 environment from the LSV curves in Figure 1, the faster flooding times indicate that activation of the carbon surface is contributing to the premature flooding mechanism of the carbon GDL. The eventual flooding of the samples in a CO_2 environment may then also be attributable to carbon activation, even if the Ag catalyst layer contributes to much of the Faradaic current density (Figure 2a). In short, the results in Figure 2 indicate that premature flooding is due to the potential-driven reduction in the capillary pressure between the electrolyte and GDL substrate. Consequently, the electrolyte wets the microporous layer (MPL) of the GDL and gradually fills in its pores while carbon in the GDL becomes active for HER.

To investigate further and indicate possible solutions to flooding, we repeated the analysis with metal catalysts that are more active than Ag for HER in an attempt to limit the reactions that occur on the carbon support. First, we performed LSVs in a N_2 environment on a variety of metal−GDL combinations (Pt, Au, and Cu). Platinum is a well-known catalyst for HER, which shows excellent activity (Figure 3a). Although the LSVs indicate the Cu/GDL and Au/GDL electrodes are not as active as the Pt/GDL, they still exhibit

https://dx.doi.org/10.1021/acsenergylett.0c02184
ACS Energy Lett. 2021, 6, 33−40

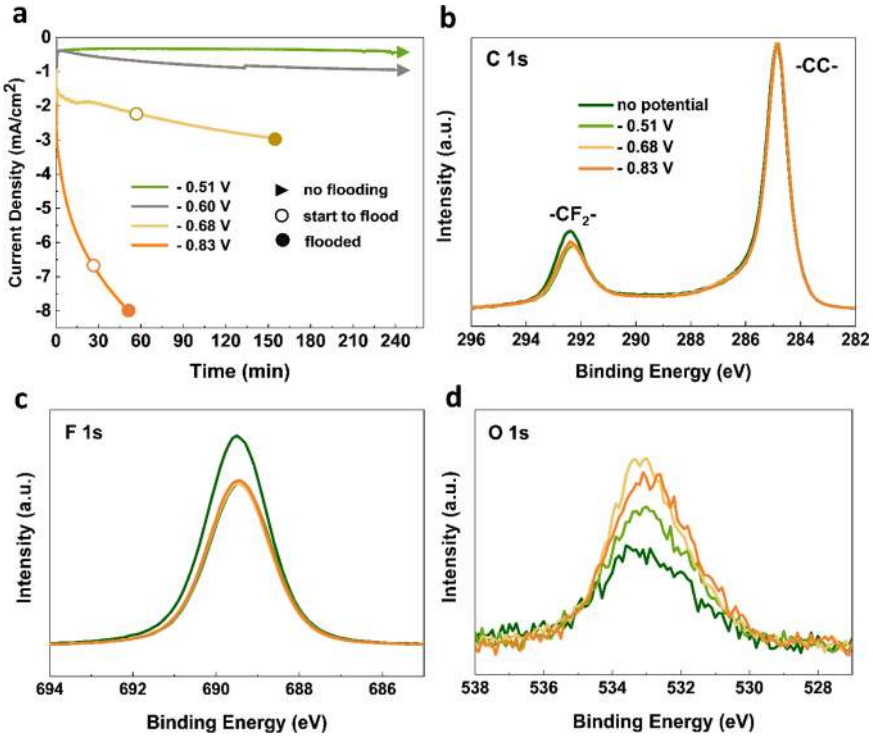

Figure 4. (a) Current densities and time when flooding happened on bare GDL at different potentials under N_2 conditions. Empty circles indicate droplet observation on the back of the GDL. Filled circles indicate droplets across the entire back of the GDL. XPS spectra of (b) C 1s, (c) F 1s, and (d) O 1s of different GDL samples.

onset potentials lower than those of the bare GDL and Ag/GDL.[33]

Chronoamperometry was then performed on these electrodes similar to the Ag/GDL samples. For the Pt/GDL electrode (Figure 3b), no droplets were observed on the back of the GDL after operation for 3 h at 10 or 50 mA/cm^2. In contrast, the Ag/GDL in a N_2 environment flooded after operation for 40 min at 10 mA/cm^2, and after only 3 min at 50 mA/cm^2. These results are explained by observing the corresponding potentials for Pt/GDL (−0.1 and −0.45 V vs RHE at 10 and 50 mA/cm^2, respectively), which are smaller than the observed onset potential for carbon to conduct HER (−0.65 V vs RHE, shown in Figures 1e and 3b). For the Cu/GDL sample, which shows HER onset potentials lower than that of the Ag/GDL but worse than that of the Pt/GDL, flooding occurred after operation for 160 min at 10 mA/cm^2. The Cu sample then showed greater resistance to flooding at a current density identical to that of the Ag/GDL. As the potential increases during operation, the applied potential becomes similar to that of the Ag/GDL, at which point flooding is observed to occur.

In a CO_2 atmosphere, the Cu/GDL and Au/GDL both have onset potentials lower than those of the Ag/GDL[34,35] and bare GDL (Figure 3c), similar to what is reported in the literature.[36,37] Chronopotentiometry in Figure 3d shows that to reach the same current density at 10 mA/cm^2, the potential needed on the Cu/GDL is less negative than on the Ag/GDL. The system was able to run for >3 h without flooding on the Cu/GDL, whereas on the Ag/GDL, flooding occurred after ∼1 h. In both N_2 and CO_2 environmenta, the potential drifted to more negative potentials on the Cu/GDL, possibly resulting from physical degradation or restructuring of the copper catalyst. Nevertheless, we cannot draw such conclusions on the basis of the SEM results, as there was no obvious morphological change after electrolysis on all GDLs (Figures S8−S10). In brief, the results from Figure 3 confirm our hypothesis that catalysts with a lower onset potential than carbon will be more resistant to flooding of the gas diffusion layer during electrochemical operation.

To further understand the role of potential and current density on flooding, we performed chronoamperometry at different fixed potentials on a bare GDL under a N_2 atmosphere in 1 M $KHCO_3$. Figure 4a shows that at applied potentials of −0.51 and −0.6 V versus RHE, no flooding was observed after operation for 4 h. The corresponding current densities for these potentials are <1 mA/cm^2. When the potential is increased to −0.68 V versus RHE, initial flooding was observed after 70 min, followed by fully dispersed flooding after 160 min. At −0.83 V versus RHE, flooding occurred at a faster rate, reaching a fully flooded state after only 50 min. Over the course of operation, the current densities are also seen to steadily increase. We anticipate the activity increase occurs due to a larger wetted surface area of carbon that is accessible for the reaction as flooding occurs (see Figure 1a). Such behavior indicates that flooding of the carbon microporous layer may be steadily occurring at the beginning of the reaction before it can be detected visually, rather than occurring suddenly. From these results, we conclude that the premature flooding mechanism requires the carbon surface to be active for HER, and that higher potentials and/or current densities on the carbon surface increase the rate of flooding.

To investigate the potential chemical change on the surface of the GDL that may cause flooding as a result of the applied potential, we performed XPS measurements on the carbon GDLs described above (Figure 4a) after chronoamperometry. The blank sample was a bare GDL, which was placed in a flow cell in the same manner as other GDLs for 4 h, but without any

https://dx.doi.org/10.1021/acsenergylett.0c02184
ACS Energy Lett. 2021, 6, 33−40

potential applied. No flooding was observed on the blank sample. Panels b−d of Figure 4 show the C 1s, F 1s, and O 1s spectra, respectively, of different GDL surfaces after normalization against C 1s (-CC- at 284.8 eV).

As a semiquantitative method, the XPS peak area represents the relative ratio of elements and thus their concentrations. Panels b and c of Figure 4 show a decrease in the C 1s (-CF_2-) and F 1s signals, while an increase in the O 1s peak on GDLs applied with potentials, compared with the blank bare GDL. Table S1 also shows a decreased surface atomic ratio of C 1s (-CF_2-) and F 1s. The F 1s ratio decreases by 12.5%, which is more obvious than C 1s due to its larger relative sensitivity factor (RSF). Such a decrease suggests that some amount of PTFE may decompose under negative potentials as reported previously (at −2 V vs SCE).[38,39] Although the potentials in our work are less negative than this, the decomposition of PTFE on the GDE can be faster than its foil/membrane form and potentially occur at more anodic potentials.[40] Once the PTFE degrades, the C−F bonds will break, and C can combine with C to form C═C bonds. Carbon can also combine with O in the electrolyte to form C−O (or C═O, etc.). A minor increase in the oxygen signals and atomic ratios were observed when potentials were applied (Figure 4d and Table S1).

It is worth mentioning that no K^+ was detected by XPS on any samples (Figure S12). Thus, we can rule out the influence of unwashed $KHCO_3$ salt on C 1s and O 1s XPS spectra. Furthermore, after the surface had been etched for 5 and 45 s, we still see decreased C 1s (-CF_2-) and F 1s peaks and an increase in the O 1s peak, respectively (Figures S13 and Figure S14). This result indicates that potential-induced GDL changes also happen in sublayers under the surface. Nevertheless, little difference is observed when comparing the C 1s and F 1s signals among −0.51, −0.68, and −0.83 V versus RHE, suggesting overall similar chemical conditions of the MPL's surface under applied potentials (a mixture of carbon and PTFE surfaces). Together with the electrochemical data, we hypothesize that water penetration may in fact be due to electrowetting effects of the exposed carbon particles, rather than a change in the structure of the MPL. Electrowetting reduces the solid−liquid interfacial tension between the carbon and electrolyte and would result in a smaller contact angle as the applied potentials become more cathodic. Via the Young−Laplace equation, the resulting capillary pressure on the carbon surface may then supersede the opposing capillary pressure of the PTFE surfaces that include a larger contact angle (θ_{PTFE} > 90°). Under this scenario, the pores of the MPL would become flooded in the presence of an applied potential (see the Supporting Information for a further description).

Of note in our work, we observed flooding of a carbon GDL in both N_2 and CO_2 environments, meaning that the flooding mechanism described here is independent of the CO_2 electrolysis conditions. In fact, under CO2RR conditions, the GDL took longer to flood than in N_2. Our proposed flooding mechanism then differs from that of the recent work by Leonard et al. that showed that the primary reason for GDL flooding was salt precipitation during CO_2 electrolysis.[21] The difference between our work and that of Leonard et al. is the use of $KHCO_3$ instead of KOH. We hypothesize that we observed different flooding mechanisms because CO2RR under alkaline conditions requires lower electrode potentials as has been shown extensively in the literature.[17,41] For example, in KOH Dinh et al.[17] reached current densities of >300 mA/cm^2 on a carbon GDL before the cathode potential reached −0.6 V versus RHE. We then expect the carbon surface to be unable to perform HER, and the potential would be low enough to avoid the flooding mechanism discussed here that occurred between −0.6 and −0.83 V versus RHE. Combined with the results from Leonard et al., we can then infer that the "first flooding mechanism" that is observed during CO_2 electrolysis is a function of the chosen electrolyte and the activity of the catalyst. In a KOH electrolyte, salt precipitation due to the total charge passed could then reasonably expected to occur before the flooding mechanism described here. It is also worth mentioning that even during electrochemical CO reduction reported by Jouny et al.,[29] where no salt formation occurs between KOH and CO, flooding was noted to be an issue when current densities were increased to 500 mA/cm^2 (the corresponding potential was approximately −0.65 V vs RHE).

To reach long-term stable operation of GDLs for CO_2 electrolysis, one way of mitigating flooding is through the continued development of catalysts with lower onset potentials, high activity, and large surface area. As demonstrated with the Pt/GDL, a sufficiently active catalyst can avoid this problem. A secondary approach can be modifying the surface of the carbon in the MPL with an additional material that is inactive for CO2RR but changes the wetting and electrochemical properties. This would have the added benefit of preventing the production of small amounts of HER from the GDL, which can slightly increase the overall CO2RR selectivity. Lastly, continued development of non-carbon GDLs is also encouraged, particularly ones that decouple the traditional requirements for a GDL (conductivity, hydrophobicity, and porosity) but remain functional over larger areas. For example, Tiwari et al. reported a Gortex-based GDE, where metallic mesh was used as the current collector to provide conductivity, while a Gortex membrane was used to provide hydrophobicity and porosity.[13] It is worth noting that our work and most others reported in the literature used commercial GDLs without any pretreatment. Further work in modifying or pretreating GDLs may prove to be useful in understanding or preventing flooding mechanisms.

In this work, we investigated the role of carbon-based GDL and applied potential on flooding during electrochemical CO_2RR. Electrochemical characterization of bare carbon and electrodes coated with various metals suggests that high negative potentials needed to drive CO2RR result in changes in the wetting characteristics of carbon-based GDL. The potential-induced flooding strongly suggests that the HER taking place on the carbon GDL accelerates the wetting of initially hydrophobic GDL. We propose that by improving catalyst activity and operating CO_2 electrolysis in a suitable (i.e., low) potential range, as well as further modifying GDL configurations, CO_2 electrolyzers would achieve longer stability. Results in this work help to improve not only stability studies at the lab scale for electrochemical CO_2 reduction but also their possibility for future applications in industry. The findings are also expected to apply to other reduction reactions (CORR and N2RR) using carbon GDEs where sufficiently high cathodic overpotentials are required.

■ ASSOCIATED CONTENT

Supporting Information

The Supporting Information is available free of charge at https://pubs.acs.org/doi/10.1021/acsenergylett.0c02184.

https://dx.doi.org/10.1021/acsenergylett.0c02184
ACS Energy Lett. 2021, 6, 33−40

A description of the experimental details, a schematic of the system, detailed LSV scans of GDL deposited with different metal catalysts under N_2 and CO_2 conditions, measurement of ECSA of PTFE and carbon-based GDLs, flooding image of the gas side of GDLs, SEM image of GDL deposited with different metal catalysts before and after the electrochemical test, chronopotentiometry test of Ag/GDL under N_2 and CO_2 conditions, and XPS data of GDLs after a chronoamperometry test at different potentials (PDF)

AUTHOR INFORMATION

Corresponding Author

Thomas Burdyny − *Materials for Energy Conversion and Storage (MECS), Department of Chemical Engineering, Faculty of Applied Sciences, Delft University of Technology, 2629 HZ Delft, The Netherlands;* orcid.org/0000-0001-8057-9558; Email: t.e.burdyny@tudelft.nl

Authors

Kailun Yang − *Materials for Energy Conversion and Storage (MECS), Department of Chemical Engineering, Faculty of Applied Sciences, Delft University of Technology, 2629 HZ Delft, The Netherlands*

Recep Kas − *Renewable and Sustainable Energy Institute (RASEI), University of Colorado, Boulder, Boulder, Colorado 80303, United States*

Wilson A. Smith − *Materials for Energy Conversion and Storage (MECS), Department of Chemical Engineering, Faculty of Applied Sciences, Delft University of Technology, 2629 HZ Delft, The Netherlands; Department of Chemical and Biological Engineering and Renewable and Sustainable Energy Institute (RASEI), University of Colorado, Boulder, Boulder, Colorado 80303, United States*

Complete contact information is available at: https://pubs.acs.org/10.1021/acsenergylett.0c02184

Notes

The authors declare no competing financial interest.

ACKNOWLEDGMENTS

K.Y. acknowledges the China Scholarship Council (CSC) for providing funding for this work. T.B. acknowledges that a portion of the project is co-financed by Shell and a PPP-allowance from Top Consortia for Knowledge and Innovation (TKI's) of the Ministry of Economic Affairs and Climate in the context of the TU Delft e-Refinery Institute. The authors also acknowledge Anirudh Venugopal, Davide Ripepi, and Bart Boshuizen for the XPS measurements and helpful discussion.

REFERENCES

(1) Hori, Y. i. Electrochemical CO_2 reduction on metal electrodes. In *Modern aspects of electrochemistry*; Springer, 2008; pp 89−189.

(2) Smith, W. A.; Burdyny, T.; Vermaas, D. A.; Geerlings, H. Pathways to Industrial-Scale Fuel Out of Thin Air from CO2 Electrolysis. *Joule* **2019**, *3* (8), 1822−1834.

(3) Fleischer, M.; Jeanty, P.; Wiesner-Fleischer, K.; Hinrichsen, O. Industrial Approach for Direct Electrochemical CO 2 Reduction in Aqueous Electrolytes. In *Zukünftige Kraftstoffe*; Springer, 2019; pp 224−250.

(4) Verma, S.; Kim, B.; Jhong, H. R. M.; Ma, S.; Kenis, P. J. A gross-margin model for defining technoeconomic benchmarks in the electroreduction of CO2. *ChemSusChem* **2016**, *9* (15), 1972−1979.

(5) Burdyny, T.; Smith, W. A. CO 2 reduction on gas-diffusion electrodes and why catalytic performance must be assessed at commercially-relevant conditions. *Energy Environ. Sci.* **2019**, *12* (5), 1442−1453.

(6) Endrődi, B.; Bencsik, G.; Darvas, F.; Jones, R.; Rajeshwar, K.; Janáky, C. Continuous-flow electroreduction of carbon dioxide. *Prog. Energy Combust. Sci.* **2017**, *62*, 133−154.

(7) Hernandez-Aldave, S.; Andreoli, E. Fundamentals of Gas Diffusion Electrodes and Electrolysers for Carbon Dioxide Utilisation: Challenges and Opportunities. *Catalysts* **2020**, *10* (6), 713.

(8) Yang, K.; Kas, R.; Smith, W. A. In situ infrared spectroscopy reveals persistent alkalinity near electrode surfaces during CO2 electroreduction. *J. Am. Chem. Soc.* **2019**, *141* (40), 15891−15900.

(9) Weng, L.-C.; Bell, A. T.; Weber, A. Z. Modeling gas-diffusion electrodes for CO 2 reduction. *Phys. Chem. Chem. Phys.* **2018**, *20* (25), 16973−16984.

(10) García de Arquer, F. P.; Dinh, C.-T.; Ozden, A.; Wicks, J.; McCallum, C.; Kirmani, A. R.; Nam, D.-H.; Gabardo, C.; Seifitokaldani, A.; Wang, X.; et al. CO_2 electrolysis to multicarbon products at activities greater than 1 A cm^{-2}. *Science* **2020**, *367* (6478), 661−666.

(11) Forner-Cuenca, A.; Biesdorf, J.; Gubler, L.; Kristiansen, P. M.; Schmidt, T. J.; Boillat, P. Engineered water highways in fuel cells: radiation grafting of gas diffusion layers. *Adv. Mater.* **2015**, *27* (41), 6317−6322.

(12) Wilkinson, D. P.; Zhang, J.; Hui, R.; Fergus, J.; Li, X. *Proton exchange membrane fuel cells: materials properties and performance*; CRC Press: Boca Raton, FL, 2009.

(13) Tiwari, P.; Tsekouras, G.; Swiegers, G. F.; Wallace, G. G. Gortex-Based Gas Diffusion Electrodes with Unprecedented Resistance to Flooding and Leaking. *ACS Appl. Mater. Interfaces* **2018**, *10* (33), 28176−28186.

(14) De Gregorio, G. L.; Burdyny, T.; Loiudice, A.; Iyengar, P.; Smith, W. A.; Buonsanti, R. Facet-dependent selectivity of Cu catalysts in electrochemical CO2 reduction at commercially viable current densities. *ACS Catal.* **2020**, *10* (9), 4854−4862.

(15) Zhang, J.; Luo, W.; Züttel, A. Self-supported copper-based gas diffusion electrodes for CO 2 electrochemical reduction. *J. Mater. Chem. A* **2019**, *7* (46), 26285−26292.

(16) Luo, W.; Zhang, J.; Li, M.; Züttel, A. Boosting CO production in electrocatalytic CO2 reduction on highly porous Zn catalysts. *ACS Catal.* **2019**, *9* (5), 3783−3791.

(17) Dinh, C.-T.; Burdyny, T.; Kibria, M. G.; Seifitokaldani, A.; Gabardo, C. M.; García De Arquer, F. P.; Kiani, A.; Edwards, J. P.; De Luna, P.; Bushuyev, O. S.; et al. CO_2 electroreduction to ethylene via hydroxide-mediated copper catalysis at an abrupt interface. *Science* **2018**, *360* (6390), 783−787.

(18) Larrazábal, G. O.; Strøm-Hansen, P.; Heli, J. P.; Zeiter, K.; Therkildsen, K. T.; Chorkendorff, I.; Seger, B. Analysis of mass flows and membrane cross-over in CO2 reduction at high current densities in an MEA-type electrolyzer. *ACS Appl. Mater. Interfaces* **2019**, *11* (44), 41281−41288.

(19) Jeanty, P.; Scherer, C.; Magori, E.; Wiesner-Fleischer, K.; Hinrichsen, O.; Fleischer, M. Upscaling and continuous operation of electrochemical CO2 to CO conversion in aqueous solutions on silver gas diffusion electrodes. *Journal of CO2 Utilization* **2018**, *24*, 454−462.

(20) De Mot, B.; Hereijgers, J.; Duarte, M.; Breugelmans, T. Influence of flow and pressure distribution inside a gas diffusion electrode on the performance of a flow-by CO2 electrolyzer. *Chem. Eng. J.* **2019**, *378*, 122224.

(21) Leonard, M. E.; Clarke, L. E.; Forner-Cuenca, A.; Brown, S. M.; Brushett, F. R. Investigating electrode flooding in a flowing electrolyte, gas-fed carbon dioxide electrolyzer. *ChemSusChem* **2020**, *13* (2), 400−411.

(22) Das, P. K.; Grippin, A.; Kwong, A.; Weber, A. Z. Liquid-water-droplet adhesion-force measurements on fresh and aged fuel-cell gas-diffusion layers. *J. Electrochem. Soc.* **2012**, *159* (5), B489.

(23) Borup, R. L.; Davey, J. R.; Garzon, F. H.; Wood, D. L.; Inbody, M. A. PEM fuel cell electrocatalyst durability measurements. *J. Power Sources* **2006**, *163* (1), 76−81.
(24) Burchardt, T. An evaluation of electrocatalytic activity and stability for air electrodes. *J. Power Sources* **2004**, *135* (1−2), 192−197.
(25) Löwe, A.; Rieg, C.; Hierlemann, T.; Salas, N.; Kopljar, D.; Wagner, N.; Klemm, E. Influence of Temperature on the Performance of Gas Diffusion Electrodes in the CO2 Reduction Reaction. *ChemElectroChem* **2019**, *6* (17), 4497−4506.
(26) Bidault, F.; Brett, D.; Middleton, P.; Brandon, N. Review of gas diffusion cathodes for alkaline fuel cells. *J. Power Sources* **2009**, *187* (1), 39−48.
(27) Hampson, N.; McNeil, A. The electrochemistry of porous electrodes: Flow-through and three-phase electrodes. *Electrochem* **1984**, *9*, 1−65.
(28) Leonard, M. E.; Orella, M.; Aiello, N.; Román-Leshkov, Y.; Forner-Cuenca, A.; Brushett, F. Flooded by Success: On the role of electrode wettability in CO2 electrolyzers that generate liquid products. *J. Electrochem. Soc.* **2020**, *167*, 124521.
(29) Jouny, M.; Luc, W.; Jiao, F. High-rate electroreduction of carbon monoxide to multi-carbon products. *Nature Catalysis* **2018**, *1* (10), 748−755.
(30) Nwabara, U. O.; Cofell, E. R.; Verma, S.; Negro, E.; Kenis, P. J. Durable cathodes and electrolyzers for the efficient aqueous electrochemical reduction of CO2. *ChemSusChem* **2020**, *13*, 855−875.
(31) Gabardo, C. M.; O'Brien, C. P.; Edwards, J. P.; McCallum, C.; Xu, Y.; Dinh, C.-T.; Li, J.; Sargent, E. H.; Sinton, D. Continuous carbon dioxide electroreduction to concentrated multi-carbon products using a membrane electrode assembly. *Joule* **2019**, *3* (11), 2777−2791.
(32) Zhang, Y.-J.; Sethuraman, V.; Michalsky, R.; Peterson, A. A. Competition between CO2 reduction and H2 evolution on transition-metal electrocatalysts. *ACS Catal.* **2014**, *4* (10), 3742−3748.
(33) Trasatti, S. Work function, electronegativity, and electrochemical behaviour of metals: III. Electrolytic hydrogen evolution in acid solutions. *J. Electroanal. Chem. Interfacial Electrochem.* **1972**, *39* (1), 163−184.
(34) Vennekoetter, J.-B.; Sengpiel, R.; Wessling, M. Beyond the catalyst: How electrode and reactor design determine the product spectrum during electrochemical CO2 reduction. *Chem. Eng. J.* **2019**, *364*, 89−101.
(35) Endrődi, B.; Kecsenovity, E.; Samu, A.; Darvas, F.; Jones, R.; Török, V.; Danyi, A.; Janáky, C. Multilayer electrolyzer stack converts carbon dioxide to gas products at high pressure with high efficiency. *Acs Energy Lett.* **2019**, *4* (7), 1770−1777.
(36) Chen, Y.; Li, C. W.; Kanan, M. W. Aqueous CO2 reduction at very low overpotential on oxide-derived Au nanoparticles. *J. Am. Chem. Soc.* **2012**, *134* (49), 19969−19972.
(37) Huang-Fu, Z.-C.; Song, Q.-T.; He, Y.-H.; Wang, J.-J.; Ye, J.-Y.; Zhou, Z.-Y.; Sun, S.-G.; Wang, Z.-H. Electrochemical CO 2 reduction on Cu and Au electrodes studied using in situ sum frequency generation spectroscopy. *Phys. Chem. Chem. Phys.* **2019**, *21* (45), 25047−25053.
(38) Barker, D.; Brewin, D.; Dahm, R.; Hoy, L. The electrochemical reduction of polytetrafluoroethylene. *Electrochim. Acta* **1978**, *23* (10), 1107−1110.
(39) Shapoval, G.; Tomilov, A.; Pud, A.; Vonsyatskii, V. Electrochemical reductive destruction of polytetrafluoroethylene. *Theor. Exp. Chem.* **1984**, *20* (2), 234−236.
(40) Schulze, M.; Bolwin, K.; Gülzow, E.; Schnurnberger, W. XPS analysis of PTFE decomposition due to ionizing radiation. *Fresenius' J. Anal. Chem.* **1995**, *353* (5−8), 778−784.
(41) Kim, B.; Ma, S.; Jhong, H.-R. M.; Kenis, P. J. Influence of dilute feed and pH on electrochemical reduction of CO2 to CO on Ag in a continuous flow electrolyzer. *Electrochim. Acta* **2015**, *166*, 271−276.

https://dx.doi.org/10.1021/acsenergylett.0c02184
ACS Energy Lett. 2021, 6, 33−40